Kinetics of the Radical−Radical Reaction, $O(^3P_J) + OH(X^2\Pi_\Omega) \rightarrow O_2 + H$, at Temperatures down to 39 K†

David Carty,‡ Andrew Goddard,§ Sven P. K. Köhler,|| Ian R. Sims,⊥ and Ian W. M. Smith*

School of Chemistry, The University of Birmingham, Edgbaston, Birmingham B15 2TT, U.K.

Received: August 8, 2005; In Final Form: October 4, 2005

The kinetics of the reaction between O atoms and OH radicals, both in their electronic ground state, have been investigated at temperatures down to ca. 39 K. The experiments employed a CRESU (*Cinétique de Réaction en Ecoulement Supersonique Uniforme*) apparatus to attain low temperatures. Both reagents were created using pulsed laser photolysis at 157.6 nm of mixtures containing H_2O and O_2 diluted in N_2 carrier gas. OH radicals were formed by both direct photolysis of H_2O and the reaction between $O(^1D)$ atoms and H_2O. $O(^3P)$ atoms were formed both as a direct product of O_2 photolysis and by the rapid quenching of $O(^1D)$ atoms formed in that photolysis by N_2 and O_2. The rates of removal of OH radicals were observed by laser-induced fluorescence, and concentrations of O atoms were estimated from a knowledge of the absorption cross-section for O_2 at 157.6 nm and of the measured fluence from the F_2 laser at this wavelength. To obtain a best estimate of the rate constants for the O + OH reaction, we had to correct the raw experimental data for the following: (a) the decrease in the laser fluence along the jet due to the absorption by O_2 in the gas mixture, (b) the increase in temperature, and consequent decrease in gas density, as a result of energy released in the photochemical and chemical processes that occurred, and (c) the formation of $OH(v = 0)$ as a result of relaxation, particularly by O_2, of OH radicals formed in levels $v > 0$. Once these corrections were made, the rate constant for reaction between OH and $O(^3P)$ atoms showed little variation in the temperature range of 142 to 39 K and had a value of $(3.5 \pm 1.0) \times 10^{-11}$ cm^3 molecule^{-1} s^{-1}. It is recommended that this value is used in future chemical models of dense interstellar clouds.

Introduction

Reactions between neutral free radicals are important in a number of environments including the atmospheres of planets,[1] especially that of Earth, combustion systems,[2] and interstellar clouds.[3] Such reactions can be divided into two categories: *association* reactions where the radicals combine to give a single molecular species and *metathetical* reactions where two species are formed as products. Both of these categories of reactions are characterized by the facts (a) that more than one potential energy surface will correlate with the reagents and (b) that reaction will occur over one or more surfaces that exhibit no energy barriers to reaction relative to the asymptotic energy of the reagents.[4]

The reaction

$$O(^3P_J) + OH(X^2\Pi_\Omega) \rightarrow O_2(X^3\Sigma_g^-) + H(^2S);\ \Delta_r H_0^\ominus = -67.2\ \text{kJ mol}^{-1} \quad \text{(R1)}$$

has emerged as a prototype for a metathesis reaction between two small free radicals. Its study has attracted considerable experimental attention,[5−9] and there have also been a large number of theoretical studies using a variety of methods including full quasiclassical trajectory calculations, variational transition state theory at the canonical and microcanonical level, statistical adiabatic channel treatments, and full scattering calculations. In this paper, we shall compare our results chiefly with the calculations of Troe and co-workers.[10] Full references to other theoretical work, that is, calculations of both potential energy surfaces and rate constants, can be found in their papers.

The most extensive experimental studies of reaction R1 have been those carried out by Smith and co-workers[5,6] and cover the temperature range from 158 to 515 K. They employed a time-resolved method in which the OH radicals were created by pulsed photolysis of a suitable precursor in excess concentrations of $O(^3P_J)$ atoms. These steady-state concentrations of atomic oxygen were generated and estimated using standard discharge-flow techniques. In the earlier work of Howard and Smith,[5] decays in the concentration of OH were followed by resonance fluorescence, whereas laser-induced fluorescence (LIF) was employed in the later experiments of Smith and Stewart.[6] The rate constants obtained by Howard and Smith and by Stewart and Smith at room temperature, k_1(298 K), and the expressions that they derived for the temperature dependence of the rate constant, $k_1(T)$, are compared in Table 1 with other experimental data obtained on this reaction since 1980. It can be seen that there is fair agreement in respect to k_1(298 K) and between the expressions derived by Lewis and Watson[7] and by Smith and co-workers for $k_1(T)$. It might be noted, in passing, that the expression for $k_1(T)$ given by Smith and Stewart

† Part of the special issue "Jürgen Troe Festschrift".

* Corresponding author. Present address: University Chemical Laboratories, Lensfield Road, Cambridge CB2 1EW, U.K. E-mail: i.w.m.smith@bham.ac.uk.

‡ Present address: Chemistry Research Laboratory, University of Oxford, Mansfield Road, Oxford OX1 3TA, U.K.

§ Present address: School of Chemistry, The University of Leeds, Leeds LS2 9JT, U.K.

|| Present address: School of Engineering and Physical Sciences, Heriot-Watt University Edinburgh, EH14 4AS, U.K.

⊥ Present address: Laboratoire PALMS, Equipe Astrochimie Experimentale, UMR CNRS-Université no. 6627, Bâtiment 11 C, Campus de Beaulieu, Université de Rennes I, 35042 Rennes Cedex, France. E-mail: ian.sims@univ-rennes1.fr.

10.1021/jp054429u CCC: $33.50
Published on Web 12/02/2005

TABLE 1: Results of Previous Kinetic Measurements (since 1980)[a] on the $O(^3P_J) + OH(X^2\Pi_\Omega) \rightarrow O_2(X^3\Sigma_g^-) + H(^2S)$ Reaction

	experimental method	T/K	$10^{11}\,k_1$(298 K)/ cm^3 molecule^{-1} s^{-1}	$10^{11}\,k_1(T)$/ cm^3 molecule^{-1} s^{-1}
Howard and Smith[5]	O atoms formed and [O] estimated using discharge-flow; OH from flash photolysis of HNO_3 and [OH] by resonance fluorescence	250−515	3.5 ± 0.3 (95%)	$3.85 \pm 0.13\ (T/298)^{-(0.50\pm0.12)}$
Smith and Stewart[6]	O atoms formed and [O] estimated using discharge-flow techniques; OH from pulsed laser photolysis of HNO_3 and [OH] observed by laser-induced fluorescence	158−294	4.2 ± 0.2 (1σ)	$f_{el} \times 3.7\ (T/298)^{-0.24\,b}$
Lewis and Watson[7]	double discharge-flow, O atoms formed and [O] estimated using standard methods, OH from $H + NO_2$ and [OH] by resonance fluorescence	221−499	3.1 ± 0.8	$3.0 \pm 1.15\ (T/298)^{-(0.36\pm0.07)}$
Brune et al.[8]	double discharge-flow, O atoms formed and [O] estimated using standard methods, OH from $H + NO_2$ and [OH] by resonance fluorescence and laser magnetic resonance		3.1 ± 0.5	
Robertson and Smith[9]	pulsed laser photolysis of O_3 and quenching of $O(^1D)$ by N_2; OH from $O(^1D) + H_2O$ and [OH] by laser-induced fluorescence	295	3.17 ± 0.51 (1σ)	

[a] Measurements prior to 1980 are summarized in ref 5b. [b] In this formulation, some of the T-dependence of the rate constant is attributed to changes in the electronic partition functions of the reagents, $O(^3P_J)$ and $OH(X^2\Pi_\Omega)$, and f_{el} is the ratio of the product of the electronic wave functions for these two species at 298 K to the same quantity, $\{5 + 3\exp(-228/T)\exp(-236/T)\}\{2 + 2\exp(-205/T)$ at temperature T.

explicitly recognized the likely effect on the rate of reaction R1 of the multiplicity of potential energy surfaces that correlate with $O(^3P_J) + OH(X^2\Pi_\Omega)$. Of these ($3^2A' + 3^2A'' + 3^4A' + 3^4A''$) surfaces, only two surfaces ($^2A'' + {}^4A''$) correlate with the reaction products $O_2(X^3\Sigma_g^-) + H(^2S)$. It is generally assumed[10] that reaction only occurs over the lowest $^2A''$ surface, which corresponds to the electronic ground state of the HO_2 transitory intermediate. Comparisons of experimental results, both those presented in this paper and those obtained previously, with theory will be postponed until the Discussion section of the present paper.

In practice, the information about the rate of reaction between OH and $O(^3P_J)$ atoms is much more extensive than might be inferred from the data provided in Table 1. The reverse reaction, that is

$$O_2(X^3\Sigma_g^-) + H(^2S) \rightarrow O(^3P_J) + OH(X^2\Pi_\Omega);\ \Delta_r H_0^\ominus = +67.2\ \text{kJ mol}^{-1} \quad \text{(R-1)}$$

has been described[2a] as one of "the two most important reactions in the combustion of hydrocarbons" and consequently has been the subject of many high-temperature studies. These data and application of the principle of detailed balance, $k_1(T)/k_{-1}(T) = K_{c,1}(T)$, where $K_{c,1}(T)$ is the equilibrium constant at temperature T, allow values of $k_1(T)$ to be calculated at temperatures up to 5300 K, meaning that there is currently laboratory kinetic data for this reaction for temperatures ranging from 158 to 5300 K.

Reaction R1 plays two important roles in atmospheric chemistry. First, coupled with the reaction

$$H + O_3 \rightarrow OH + O_2;\ \Delta_r H_0^\ominus = -324.5\ \text{kJ mol}^{-1} \quad \text{(R2)}$$

it forms one of the catalytic cycles that remove "odd oxygen" in the upper stratosphere.[11a] Second, the same pair of reactions occur in the high mesosphere between about 70 and 90 km altitude, and the strongly exothermic reaction (R2) forms OH in high vibrational levels ($v \leq 9$), giving rise to the Meinel bands, which are high overtone vibrational transitions in OH.[11b]

The reaction between OH radicals and atomic oxygen has a central role in what is referred to as the "interstellar O_2 problem": the fact that there appears to be much less molecular oxygen than expected in interstellar environments, especially in the cold cores of dark interstellar clouds (ISCs) where early steady-state models[12] predicted that O_2 should have a similar abundance as CO. At that time, it was thought that reaction R1 should be the main sink of OH and the main producer of O_2, at least in the molecular cloud TMC-1. Of course, the spectroscopic observation of interstellar O_2 presents two special problems. First, as a homonuclear diatomic molecule, there are no electric-dipole-moment-induced transitions between neighboring rotational levels so that one must rely on much weaker magnetic-dipole-induced transitions,[13] either those with $\Delta N = 2$, such as $N_J = 3_3 \rightarrow 1_2$ or those between different spin states of the same rotational level, such as $N_J = 1_1 \rightarrow 1_0$. Second, the presence of abundant O_2 in Earth's atmosphere makes observations by ground-based instruments particularly difficult.

Attempts to address the second of these problems include the following: (i) attempts to observe lines from $^{16}O^{18}O$,[14] (ii) efforts to observe extra-galactic $^{16}O_2$ with sufficient red-shift to ensure that the frequencies emitted will not coincide with absorption frequencies in Earth's atmosphere,[15] and (iii) the use of balloon-borne instruments.[16] All of these experiments have failed to observe definite spectroscopic signatures of O_2 and have led to estimates of upper limits of the O_2 abundance in various astronomical sources lower than that expected on the basis of early steady-state models.

Within the past few years, there have been two major efforts to search for interstellar O_2 using satellite-based instruments. The sub-millimeter wave astronomy satellite (SWAS) mission was launched into low Earth orbit in late 1998. It attempted to observe O_2 using the $N_J = 3_3 \rightarrow 1_2$ transition at 487.2494 GHz. No convincing detection of O_2 from 20 potential sources was reported, and a combination of data from 9 sources indicated an abundance relative to H_2 of $N(O_2)/N(H_2) \leq (0.33 \pm 1.6) \times 10^{-7}$ at the 3σ level.[17] The Odin mission, launched in 2001, was capable of making measurements at the same frequency as SWAS, but concentrated on measurements at 118.750343 GHz, the frequency of the $N_J = 1_1 \rightarrow 1_0$ transition, in part because the upper level of this line has a lower excitation energy (equivalent to 5.7 K) than that of the upper level of the $N_J = 3_3 \rightarrow 1_2$ transition (equivalent to 26.4 K). Initially, no definite sighting of O_2 could be reported and the upper limits of the O_2 abundance were lowered still further: by factors of 20 and 40 for L134N and TMC-1, respectively.[18] However, more recently Liseau and co-workers[19] have reported the detection of O_2 toward the dense molecular core *ρOphA*, which is part of a

region of active star formation. This observation suggests an abundance of the order of 10^{-7}. Confirmation must await the deployment of further instruments such as the Herschel-HIFI facility.

In the short time since the SWAS results were reported, there have been a number of other modeling studies[20−24] designed to explain the unexpectedly low abundances of O_2 that are apparently present in interstellar sources. Among the speculative reasons advanced for the surprisingly low upper limits to observed O_2 abundances have been the following: (i) a larger than expected rate for the photodestruction of O_2;[20] (ii) "clumpiness" of the structure in which inhomogeneity of ISCs allows the residual UV radiation field in the cores to destroy O_2 by photodissociation;[21] (iii) accretion onto dust grains, a model that achieved reasonable agreement with the SWAS results at times of one to two million years after the formation of the cloud;[22] and (iv) turbulence or some other factor leading to the interior of the observed sources being "chemically young".[24] However, Wilson et al.[25] report a very recent attempted detection of O_2 by Odin in the small magellanic cloud (SMC), which also proved negative, and they argue that such chemically young models are ruled out in the SMC.

Finally, and of most direct relevance to the present work, Viti et al.[23] discussed the role of the reaction between OH radicals and O atoms as the primary source of molecular oxygen. They took values of $k_1(T)$ from the database held at UMIST,[26] which gave, for example, a value of $k_1(40\ \mathrm{K}) = 5.6 \times 10^{-11}$ $\mathrm{cm^3\ molecule^{-1}\ s^{-1}}$. However, they explored the effect on their calculations of assuming an activation energy for the reaction that would be too small to have much effect on the experimental measurements at $T \geq 158$ K,[6] but which would reduce the rate of reaction 1 at the temperatures (10−20 K) of dark, dense ISCs. They concluded that an activation energy equivalent to about 80 K would be consistent with the measurements of Smith and Stewart[6] and lower the rate in ISCs to bring the abundance of O_2 into agreement with the SWAS observations.

The contentious role of reaction R1 in the chemistry of interstellar clouds was a major motivation for our present attempts to extend the measurements of $k_1(T)$ to lower temperatures than hitherto. A second stimulus was the challenge to devise a method, which allowed the rate of reaction between two unstable neutral radicals to be determined at very low temperatures, for the first time. To attain these low temperatures, we made use of the Birmingham CRESU (*Cinétique de Réaction en Ecoulement Supersonique Uniforme*) apparatus.[27] The substantial gas flows in a CRESU apparatus, and other reasons, made it impossible to generate sufficient $O(^3P_J)$ atoms by the discharge methods employed previously.[5,6] Consequently, both reagents have been generated photochemically in such a way that the initial concentration of oxygen atoms was much greater than that of hydroxyl radicals; that is, $[O(^3P)]_0 \gg [OH]_0$. Thus, the concentration of OH, observed by laser-induced fluorescence (LIF), decayed essentially by pseudo-first-order kinetics. The photolysis source was an F_2 excimer laser operating at 157.6 nm. The radiation from this laser photolyses O_2

$$O_2 + h\nu\ (\lambda = 157.6\ \mathrm{nm}) \rightarrow O(^3P) + O(^1D);\ \Delta_r H_0^{\ominus} = -75.7\ \mathrm{kJ\ mol^{-1}} \quad \text{(R3)}$$

and the $O(^1D)$ atoms are quenched rapidly by O_2 and the N_2 carrier gas

$$O(^1D) + O_2, N_2 \rightarrow O(^3P) + O_2, N_2;\ \Delta_r H_0^{\ominus} = -189.8\ \mathrm{kJ\ mol^{-1}} \quad \text{(R4)}$$

A small concentration of OH radicals is created by inclusion of a small mole fraction of H_2O in the gas mixture. Some of this is photolyzed and some reacts with a small fraction of the $O(^1D)$ atoms produced by photolysis of the O_2

$$H_2O + h\nu(\lambda = 157.6\ \mathrm{nm}) \rightarrow OH(X^2\Pi) + H;\ \Delta_r H_0^{\ominus} = -257.2\ \mathrm{kJ\ mol^{-1}} \quad \text{(R5)}$$

$$O(^1D) + H_2O \rightarrow 2\ OH(X^2\Pi);\ \Delta_r H_0^{\ominus} = -123.8\ \mathrm{kJ\ mol^{-1}} \quad \text{(R6)}$$

The lowest temperature that can be generated using the Laval nozzles that we have for operation with N_2 as the carrier gas is 39 K. The use of nozzles designed to operate with He at lower temperatures would mean that the quenching of $O(^1D)$ atoms to $O(^3P)$ atoms is likely to be unacceptably slow.

Experimental Method

The current experiments were performed using the Birmingham CRESU apparatus, which has been described in some detail elsewhere.[27] Interchangeable Laval nozzles lie at the heart of a CRESU apparatus. They control the expansion of the gas in order to achieve uniform density and temperature in the supersonic jet downstream of the nozzle exit. Each nozzle is designed to achieve a particular temperature and density for the chosen carrier gas. In the present work, to bring about rapid quenching of the $O(^1D)$ atoms created in the photodissociation of O_2, we only employed nozzles that were designed to work with N_2 as the carrier gas. These nozzles allowed us to access temperatures of 39, 47, 83, and 142 K. For the present experiments, the main modification to the CRESU apparatus was to the plate at the downstream end of the main chamber. This was changed to allow us to introduce radiation from a VUV F_2 excimer laser (Lambda-Physik, LPX 210i). This radiation, at a wavelength of 157.6 nm and propagating counter to the gas jet, photolyzed both the O_2 and H_2O that were included in the gas flow.

The F_2 excimer laser was fitted with unstable resonator optics to minimize the divergence of the beam over its long path length both external to and within the main CRESU chamber. With these laser optics in place, it proved unnecessary to employ any collimating optics between the exit of the laser and the point where the laser beam entered the CRESU chamber. To reduce attenuation of the beam by atmospheric absorption on its path to the chamber, it was passed through tubes that were flushed with high-purity Ar. The final arm of this delivery system passed through the end plate of the CRESU chamber, terminating about 10 cm before the observation point from which LIF signals were gathered, and was closed with a MgF_2 Brewster's angle window. The argon flushing these pipes was admitted at the end closest to the exit of the excimer laser and exited close to the window through which the 157.6-nm radiation entered the CRESU chamber.

N_2 carrier gas and O_2 were introduced into the reservoir upstream from the Laval nozzle via calibrated mass flow controllers (MKS Instruments Ltd.) of 100 and 20 standard liters per minute (74.4 and 14.9 mmol s^{-1}) capacity, respectively. A very small mole fraction of H_2O was included in the gas mixture by diverting a small fraction of the N_2 flow and bubbling it through distilled H_2O before this flow was mixed with the other gases in the gas reservoir.

OH radicals were detected by excitation in the (1, 0) band of the $A^2\Sigma^+ - X^2\Pi$ system. Laser radiation at a wavelength of ca. 282 nm was generated using the frequency-doubled output of a

Nd:YAG laser (Continuum, Powerlite Precision II) to pump a dye laser (Laser Analytical Systems, LDL 20505) operating with Rhodamine 6G dye (Exciton) in methanol, the output of which was frequency doubled in a BBO crystal. This probe laser beam entered the CRESU main chamber and gas reservoir through two quartz Brewster windows and passed through the Laval nozzle throat and down the gas flow along its axis counter to the direction of the photolysis beam. Fluorescence from OH-($A^2\Sigma^+$, $v = 0$ and 1) was gathered by an efficient optical system, passed through a narrow band interference filter centered at 310 nm with a fwhm of 10 nm, and was detected by a photomultiplier tube (Electron Tube Ltd., 9125 MGFLB). The signal from the PMT was recorded by a gated integrator and boxcar averager (Stanford Research Systems) and transferred to a PC via an IEEE interface (Stanford Research Systems, SR 245) controlled by data acquisition software. The time delay between the pump and probe beams, which was scanned to generate decay traces, was controlled by a four-channel delay/pulse generator (Stanford Research Systems, DG535), which was also controlled by the same data acquisition software via an IEEE interface. The DG535 also set the trigger timings of the lasers.

Proper overlap between the two laser beams was ensured by first aligning the 282-nm beam from the probe laser using irises at either end of the chamber. The beam from the excimer laser was then aligned making use of a quartz plate, which was coated on the side nearest the F_2 laser with sodium salicylate and mounted in front of the nozzle. This allowed the fluorescence generated by both lasers to be observed once the chamber had been evacuated. The gas reservoir and nozzle could then be adjusted to ensure good overlap between the two beams. After good alignment of the two beams was achieved, an iris of 4-mm-diameter (just larger than the beam from the probe laser) was mounted in front of a sensitive joulemeter (Molectron Ltd.) and this assembly was mounted in front of the Laval nozzle. The chamber was then evacuated and the fluence of the 157.6 nm photolysis laser was measured at different longitudinal positions of the reservoir and nozzle. The joulemeter had previously been calibrated against a powermeter (Molectron Ltd.) calibrated for 157.6 nm so that the readings from the joulemeter could be converted into a fluence easily. The fluence was measured before each series of experiments. It was generally in the range 15−20 mJ cm^{-2}. Although this measurement of laser fluence was repeated many times, its uncertainty could be a significant source of error in estimating the concentrations of O atoms, and therefore in the derived rate constants.

Data Analysis

In the standard experiment on the kinetics of a neutral−neutral reaction in a CRESU apparatus, a small concentration of the radical species is produced along the axis of the flow by pulsed laser photolysis of a suitable precursor. The gas in the jet is "optically thin" so that the radical concentration that is formed is essentially independent of the position along the axis of the jet. Decays in the radical concentration as a result of reaction are measured in the presence of different excess concentrations of the co-reagent and yield pseudo-first-order rate constants (k_{first}). The concentration of the co-reagent in each experiment can be obtained from the gas flows of the individual species in the gas mixture and the total gas density in the jet. Sufficient co-reagent can be added to ensure that the radical concentration is reduced to effectively zero during the time available for measurement; that is, the time it takes for gas in the jet to move from the exit of the Laval nozzle to the point near the downstream end of the uniform flow at which relative radical concentrations are measured.

The ideal situation described in the previous paragraph could not be achieved in the present experiments, where the co-reagent, $O(^3P)$ atoms, were created by photolysis of O_2. In particular, to generate sufficient $O(^3P)$ atoms to ensure that reaction R1 appreciably reduced the concentration of OH radicals during the observation time, the concentration of O_2 in the gas jet had to be so large that the intensity of the radiation from the photolysis laser was reduced as it passed along the axis of the jet. This meant that the concentrations of both OH and $O(^3P)$ created at $t = 0$ (when the excimer laser fires) depended on the position along the jet. Then, if x measures the distance upstream from the observation point, these initial concentrations are given by the equations

$$[OH]_{t=0,x} = [OH]_{t=0,x=0} \exp\{-(\sigma x[O_2] - \alpha x)\} \quad (1a)$$

and

$$[O(^3P)]_{t=0,x} = [O(^3P)]_{t=0,x=0} \exp\{-(\sigma x[O_2] - \alpha x)\} \quad (1b)$$

In these equations, the first term in the exponent is derived from the Beer−Lambert law and describes the reduction of $[OH]_{t=0,x}$ and $[O(^3P)]_{t=0,x}$ upstream from the observation point ($x = 0$) as the photolysis laser was absorbed by a concentration, $[O_2]$, of molecular oxygen in the flow.[28] The second term in the exponent is included to allow for any variations in the fluence of the photolysis beam along the axis of the gas jet.[29] The value of parameter α was determined by measuring the decay in the LIF signal when OH was created by photolysis of a small concentration of H_2O in N_2, with no O_2 present. In these experiments, performed before each series of kinetic measurements, the variation in signal with time entirely reflected the variable amount of OH formed along the axis of the gas jet due to the divergence, convergence, or slight misalignment of the photolysis laser, diffusional loss of OH being negligible under our experimental conditions, where the probe laser observes changes in the OH concentration along a narrow central portion of the much larger volume illuminated by the photolysis laser. Once allowance is made for reduction in the initial concentration of O atoms as a result of expansion following the release of energy in the photolysis of O_2, reaction R3, and the quenching of $O(^1D)$ atoms in reaction R4 (see below), further diffusion of O atoms on the time scale of the experiments was insignificant. In addition, we note that atomic recombination of $O(^3P)$ atoms and their combination with O_2 will be far too slow to reduce their concentration on the time scale of the present experiments.[30]

With O_2 in the gas mixture and $O(^3P)$ atoms formed by photolysis of O_2, the rate expression for the disappearance of OH radicals at any point along the axis in the (moving) gas jet as the reaction proceeds is

$$-d[OH]_{t,x}/dt = k_{1st,x}[OH]_{t,x} \text{ where } k_{1st,x} = k_1[O(^3P)]_x \quad (2)$$

The concentration of atomic oxygen depends on x because of absorption of the photolysis laser by O_2 and variation of the laser fluence, as expressed by eq 1b, but not on t because $[O(^3P)]_{t=0,x} \gg [OH]_{t=0,x}$; that is, the experiments were performed under pseudo-first-order conditions. So we can write

$$[O(^3P)]_x = [O(^3P)]_{t=0,x=0} \exp\{-(\sigma x[O_2] - \alpha x)\} \quad (3)$$

and substitution into eq 2 and integration yields

$$[OH]_{t,x} = [OH]_{t=0,x=0} \exp\{-(\sigma x[O_2] - \alpha x)\} \times \exp\{-(k_1[O(^3P)]_{t=0,x=0}t) \exp\{-(\sigma x[O_2] - \alpha x)\}\} \quad (4)$$

Next, we note that x and t are connected by the relationship $x = vt$, where v is the velocity of the flow in the jet. Consequently, eq 4 can be transformed into one involving time as the only variable

$$[OH]_{t,x=0} = [OH]_{t=0,x=0} \exp\{-(\sigma[O_2] - \alpha)vt\} \times \exp\{-(k_1[O(^3P)]_{t=0,x=0}t) \exp\{-(\sigma [O_2] - \alpha\, vt)\}\} \quad (5)$$

The intensity of the LIF signals observed at $x = 0$ is proportional to $[OH]_{t,x=0}$, so the variation of these signals as the time delay between the pulses from the photolysis and probe lasers is varied and fitted to an expression of the form

$$f(t) = a \exp(-bt) \exp(-k_{1st}t \exp(-bt)) + c \quad (6)$$

where a corresponds to the LIF signal at zero delay, $b = (\sigma[O_2] - \alpha)\, v$, and c corresponds to the value of the signal prior to the pulse from the photolysis laser. LIF decay traces were fitted to this form, using estimated values of b, to yield values of k_{first} .

A second-order plot of k_{first} versus $[O(^3P)]_{x=0}$ then yields a straight line where the gradient is the desired second-order rate constant, k_1. The $O(^3P)$ atom concentration at $x = 0$ was estimated from (i) the known concentration of O_2 included in the gas mixture, (ii) the measured fluence (F in J cm^{-2}) from the photolysis laser at the observation point, and (iii) the absorption cross-section of O_2 (σ_{O_2}) at $\lambda = 157.6$ nm of 5.94×10^{-18} cm^2.[28] The required atom concentration is given by

$$[O(^3P)]_{x=0} = \{F\lambda/hc\}\sigma_{O_2}\, 2[O_2] \quad (7)$$

where c is the speed of light and h is Planck's constant, so that $\{F\lambda/hc\}$ is the number of photons from each pulse of the photolysis laser incident on 1 cm^2.

There are two other possible causes of systematic error that might arise in the present experiments. The first is the temperature rise, and consequent reduction in gas density, that might have occurred as the result of the exothermic photochemical and chemical processes represented by eqs R3−R6. The second arises because the method used to generate OH radicals, that is, processes R5 and R6, do not produce OH only in its lowest vibrational level. Consequently, vibrational relaxation of OH($v > 0$), occurring on the same time scale as removal of OH($v = 0$) by reaction, might have complicated the kinetics of OH($v = 0$) and thus caused the derived value of k_1 to differ from its true value. These two aspects of our experiments are discussed further in the Discussion section of this paper.

Results

Figure 1 shows examples of two traces of the LIF signal from OH against the delay time between the pulses from the photolysis and probe lasers in experiments where the temperature initially produced in the gas jet is 47 K. Panel a shows the result of an experiment with a low concentration of O_2, and therefore of O atoms; panel b with higher concentrations of O_2, and therefore more O atoms present. The experimental data were fitted to eq 6, as described in the previous section to yield values of $k_{\text{first}} = k_1[O(^3P)]_{x=0}$. This fit was started after delays of 50 μs to allow for relaxation of any nonthermal populations over rotational levels in OH and spin−orbit levels in both OH and $O(^3P_J)$ atoms. The derived values of k_{first} were then plotted against $[O(^3P)]_{x=0}$ as shown in Figure 2 to find values of k_1 for the particular temperature of that series of experiments. Finally, the values of k_1 at different temperatures are shown in the penultimate column of Table 3, headed k_1(uncorr.), and the variation of k_1(uncorr.) with temperature is shown in Figure 3.

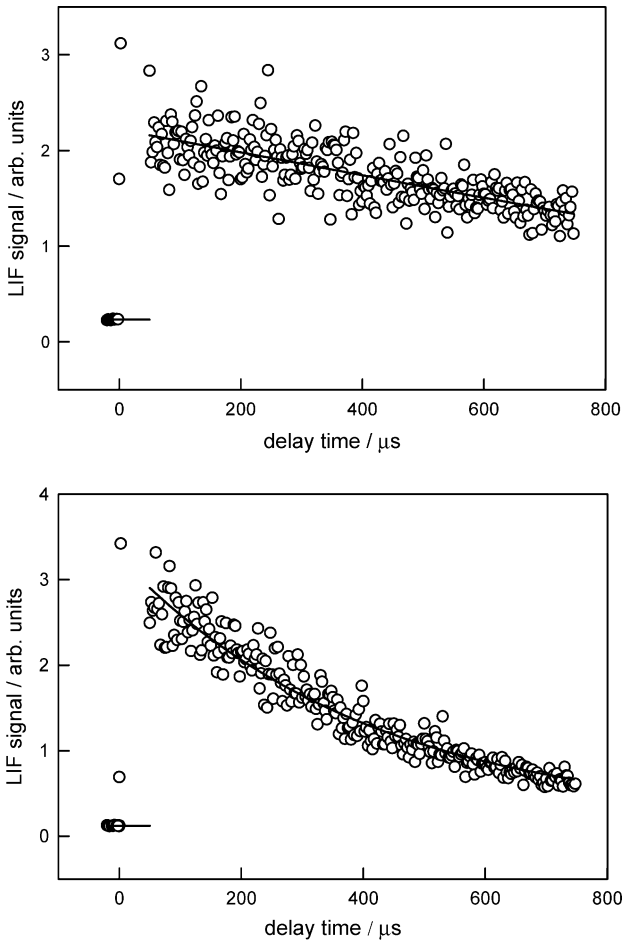

Figure 1. LIF signals from OH at different delay times between the pulses from the photolysis and probe lasers. Both traces are recorded at 47 K. In the upper panel, $[O(^3P)] = 5.4 \times 10^{13}$ molecule cm^{-3}; in the lower panel, $[O(^3P)] = 13.9 \times 10^{13}$ molecule cm^{-3}.

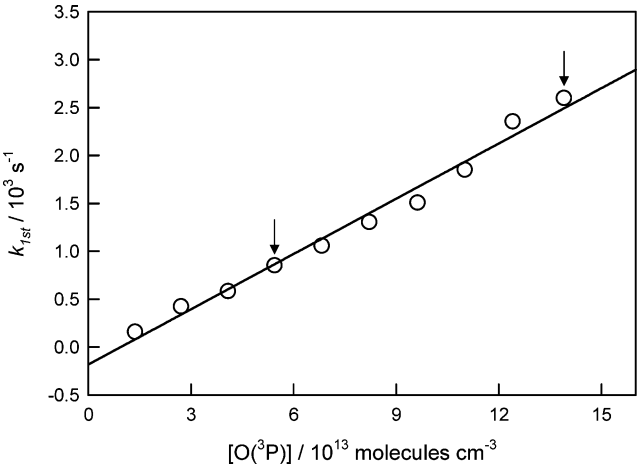

Figure 2. Plot of the pseudo-first-order rate constants (k_{first}) for decay of the OH concentration at 47 K plotted against the concentration of $O(^3P)$ atoms, uncorrected for the heating effect considered in the Discussion section of this paper. The statistical errors, arising from fitting the decay curves to eq 6, are smaller than the size of the points. The arrows indicate the values of k_{first} derived from the fits shown in Figure 1.

Two experimental runs were performed at each temperature, except 39 K. This allowed some idea of the reproducibility of the experiments to be gained. The spread in the rate constants

TABLE 2: Rate Constants, $k_1(T)$, for the Reaction between $O(^3P_J)$ Atoms and $OH(X^2\Pi_\Omega)$ Radicals

T/K[a]	$[N_2]/10^{16}$ molecule cm^{-3}	$[O_2]/10^{14}$ molecule cm^{-3}	$[O(^3P)]/10^{13}$ molecule cm^{-3}	number of points	k_1(uncorr.)/10^{-11} cm^3 molecule^{-1} s^{-1}	k_1(corr.)/10^{-11} cm^3 molecule^{-1} s^{-1}
142−160	8.80	1.82−18.6	3.37−34.4	10	3.43 ± 0.7	4.22 ± 1.3
142−161	8.80	1.86−18.9	3.64−37.0	10	2.61 ± 0.5	3.25 ± 1.0
83−99	4.88	0.43−8.67	0.86−17.3	11	2.61 ± 0.5	3.20 ± 1.0
83−93	4.88	0.86−8.78	1.08−11.0	10	2.85 ± 0.6	3.82 ± 1.1
47−71	2.65	0.64−6.55	1.34−13.8	10	1.92 ± 0.4	3.20 ± 1.0
47−71	2.65	0.65−6.63	1.36−13.9	10	2.72 ± 0.55	3.92 ± 1.2
39−48.5	3.33	0.29−3.49	0.58−7.02	13	2.50 ± 0.5	3.42 ± 1.1

[a] the temperature on the left is that created in the supersonic flow as a result of the hydrodynamic expansion; that on the right is the temperature calculated on the basis of heat released during the formation of $O(^3P)$ atoms by photolysis of O_2 and quenching of $O(^1D)$ atoms for the largest addition of O_2 in each set of experiments.

TABLE 3: Rate Constants Used in Modeling Calculations

process	$k(T)$/cm^3 molecule^{-1}s^{-1}
$H_2O + h\nu$ ($\lambda = 157.6$ nm) → OH(v) + H	where $f(0)$: $f(1)$: $f(2)$: $f(3)$: $f(4) = 0.31$: 0.35: 0.19: 0.094: 0.047
$O(^1D) + H_2O \rightarrow OH(v) + OH(0)$	$f(v) \times 2.0 \times 10^{-10}$ where $f(0)$: $f(1)$: $f(2) = 0.69$: 0.22: 0.09
$O(^1D) + N_2 \rightarrow O(^3P) + N_2$	2.6×10^{-11}
$O(^1D) + O_2 \rightarrow O(^3P) + O_2$	2.6×10^{-11}
$OH(v = 1-4) + O(^3P) \rightarrow O_2 + H$	3.2×10^{-11}
$OH(v = 1-4) + O(^3P) \rightarrow OH(v-1) + H$	1.3×10^{-11}
$OH(v = 1-4) + O_2 \rightarrow OH(v-1) + O_2$	$(v = 1)$: 7.5×10^{-14} $(T/298)^{-1.4}$
	$(v = 2)$: 1.1×10^{-13} $(T/298)^{-1.4}$
	$(v = 3)$: 5.3×10^{-13} $(T/298)^{-1.4}$
	$(v = 4)$: 8×10^{-13} $(T/298)^{-1.4}$
$OH(v = 1-4) + N_2 \rightarrow OH(v-1) + N_2$	$(v = 1)$: 1.5×10^{-15}
	$(v = 2)$: 6.0×10^{-15}
	$(v = 3)$: 2.1×10^{-14}
	$(v = 4)$: 3.0×10^{-14}

(that is, the average discrepancy from the mean of the two values) is 11, 4, and 17% for experiments at 142, 83, and 47 K, respectively. On the basis of these figures, the statistical errors in fitting the LIF traces and in the plots of k_{first} versus $[O(^3P)]$, and the likely uncertainties in estimating the fluence of the photolysis laser and hence in the estimates of $[O(^3P)]_{x=0}$ (but not any systematic error because of an incorrect value of σ_{O_2}), we ascribe an error of 20% to our derived values of k_1. Two other sources of systematic error are considered, and corrected for, in the next section.

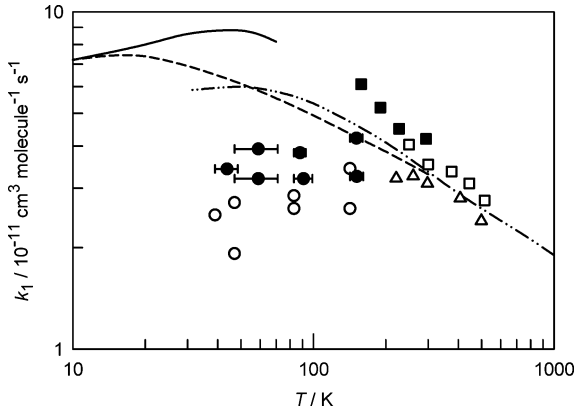

Figure 3. Comparison of temperature-dependent experimental and theoretical data for the reaction between OH radicals and $O(^3P)$ atoms. The present uncorrected and corrected values of k_1 are shown as open (○) and closed (●) circles, respectively. The corrected values of the rate constants are plotted at a temperature at the midpoint of the range indicated in Table 2, with the horizontal lines through the points indicating the range of estimated temperatures. The data of Howard and Smith[5] and Smith and Stewart[6] are represented by open (□) and filled (■) squares, respectively, and those of Lewis and Watson[7] by open triangles (△). The lines represent theoretical results: − − −, the recommended rate expression of Davidsson and Stenholm;[34] — —, the quantum SACM calculations of Troe and Ushakov;[10c] — · · — · ·, the classical trajectory calculations of Troe and Ushakov.[10c]

Discussion

We begin this section by considering two potential sources of systematic error that were mentioned at the end of the section on Data Analysis but not allowed for in deriving the values of k_1(uncorr.) listed in the penultimate column of Table 3.

(a) Effects of Energy Release as a Result of the Photochemical Formation of O(3P) Atoms. In most kinetics experiments, where pulsed laser photolysis is used to generate free radicals, it is possible to add sufficient inert "buffer" gas to ensure that there is no rise in temperature as a result of the photochemical and subsequent chemical processes in the system. This is the situation in previous CRESU experiments on neutral−neutral reactions of atoms and free radicals because the concentration of the unstable atom or radical that could be observed, usually by LIF, was very small and the dilution of the radical precursor in the carrier gas was sufficient to maintain a constant temperature.

However, in the present experiments, the co-reagent, $O(^3P)$ atoms, as well as the observed radical OH, was formed by photolysis and it is necessary to consider carefully the effect of the heat released in reactions R3 and R4. (Although reactions R5 and R6 are also exothermic, the concentration of H_2O included in the gas mixture was much less than that of O_2, so the energy released in these processes can be neglected.) Our assessment of the effects of this heat release on the temperature in the gas and on our measurements of k_1 proceeds in stages. First, we consider the heat released per unit volume (q) as a result of processes R3 and R4. Second, we divide the heat released by the heat capacity of the gas per unit volume at constant pressure (C_p) to find an increase in temperature ($\Delta T = q/C_p$). We then assume that the irradiated gas expands (instantaneously) so that its density, and particularly the concentration of O atoms, falls by a factor $T/(T + \Delta T)$. Finally, the value of k_1(uncorr.) is multiplied by a factor allowing for the effective reduction in O atom concentrations in a particular

series of experiments. The first column in Table 2 indicates the temperature range for each set of experiments: the first temperature given is that produced in the gas jet by the hydrodynamic expansion, the second temperature is that estimated on the basis of instantaneous release of heat in the experiment in each set in which the largest concentration of O_2 was included in the gas mixture.

To clarify these calculations, we take one example, using the conditions of the experiment at 39 K with the highest addition of O_2 ($[O_2] = 3.49 \times 10^{14}$ molecule cm^{-3}). Close to 10% of the O_2 is photodissociated yielding 7.02×10^{13} molecule cm^{-3} of O atoms and releasing, via R4 and R5, $q = 1.51 \times 10-5$ J cm^{-3}. The required heat capacity, C_p, for a sample of N_2 at a density of 3.33×10^{16} molecule cm^{-3} is $1.61 \times 10-6$ J K^{-1} cm^{-3}, so the predicted rise in temperature, ΔT, equals 9.5 K. Thus, after expansion of the gas, the [O(^{3}P)] concentration is 0.80 of its nominal value.

Because the rate constant, k_1, is quite invariant with temperature, the main effect of the temperature increase was the resultant decrease in the O atom concentration. The overall effect was to alter $[O(^3P)]_{x=0}$ in each experiment from the value first estimated and hence to change the gradient of plots such as that shown in Figure 2, thereby increasing the value of k_1 above the value originally estimated. The factor correcting for the effects of heat released as a result of the photochemical formation of O(^{3}P) atoms, as a result of processes R3 and R4, varied between 1.12 and 1.49.

(b) Effects of the Formation and Vibrational Relaxation of OH($v > 0$). In contrast to the studies of Howard and Smith[5] and of Smith and Stewart,[6] where flash photolysis of H_2O and pulsed laser photolysis of HNO_3 at 266 nm, respectively, were used to generate OH predominantly in the ($X^2\Pi$, $v = 0$) level, in the present experiments we had to use processes R5 and R6, which generate OH radicals over a range of vibrational levels.[31,32] In general, the production of vibrationally excited species need not complicate the kinetic analysis of the ($v = 0$) concentration in two limiting cases: first, when vibrational relaxation is much *faster* than the reactive removal of the radical from ($v = 0$) and, second, when the vibrational relaxation is much *slower* than the reaction. Unfortunately, neither of these situations pertained in the present experiments. The rate of relaxation of OH($v > 0$), predominantly in collisions with O_2, is, as far as we can determine, comparable in speed to the removal of OH($v = 0$) by reaction with O(^{3}P) atoms. Therefore, to estimate the effect of this relaxation on our analysis of the reactive kinetics, we have carried out some modeling calculations using the kinetic modeling program FACSIMILE.[33]

These FACSIMILE calculations made use of the kinetic data listed in Table 3. The vibrational distributions of OH from photolysis of H_2O and from the reaction of O(^{1}D) with H_2O were taken from the work of Hwang et al.[31] on the photolysis of H_2O, and from the studies of Gericke et al.[32a] and Cleveland and Wiesenfeld,[32b] of the reaction of O(^{1}D) with H_2O. Comparison of the strength of the LIF signals from OH with and without O_2 present showed that, when O_2 was present, the majority of the OH in our experiments came from reaction R6, in agreement with the modeling predictions. Vibrational relaxation of OH($v > 0$) was assumed to occur in single quantum steps; for example

$$OH(v) + O_2 \rightarrow OH(v-1) + O_2 \qquad (R7)$$

The main relaxant was O_2, which is surprisingly efficient in relaxing vibrationally excited OH, possibly because of a moderately strong attractive interaction between OH radicals and O_2.[34] To estimate rate constants for relaxation of different vibrational levels ($v = 1-4$) of OH by O_2 and N_2, we made use of the data reported for $T = 294$ K by D'Ottone et al.,[35] which is in fairly good agreement with earlier results on the vibrational relaxation of OH by O_2 and N_2.[36] To provide rate constants for relaxation at low temperatures, we assumed that the negative temperature-dependence reported by McCabe[37] for OH($v = 1$) with O_2 at temperatures between 371 and 205 K holds down to 39 K and is the same for vibrational levels up to $v = 4$. We have further assumed that the rate constants for relaxation by N_2 do not vary with temperature.

FACSIMILE calculations were performed to generate concentrations of OH($v = 0$) at different delays. These concentrations were fitted to a single exponential by varying the value of k_1 to find the best fit. Table 3 shows the value of k_1 ($k_{1,\text{input}}$) that was generally employed as input to the Facsimile program. The relative importance of reaction and relaxation in collisions between OH(v) radicals and O(^{3}P) atoms was assumed to be the same for all v, and we took the value used by Robertson and Smith.[9] The results of the calculations are not sensitive to the choice of this ratio. We found that it was unnecessary to perform more than one calculation in order to obtain a good fit to the data.

Calculations of the kind described were carried out for the lowest and highest O(^{3}P) concentrations in each series of experiments. This enabled us to estimate a correction factor for each series of experiments by comparing the difference in the first-order rate constants for the highest and lowest [O(^{3}P)] with and without the production and relaxation of OH($v > 0$) allowed for. This correction factor varied between 1.10 and 1.15 for the experiments listed in Table 3. These correction factors were multiplied by those allowing for a density increase because of the heat released in the same set of experiments, and the result was used to convert the values of k_1(uncorr.) to our final best estimates of k_1, that is, k_1(corr.), the values that are given in the final column of Table 3. We tested the sensitivity of the results of these calculations to the assumed values of the relaxation rate constants by repeating the calculations with these rate constants doubled and then halved. This procedure showed that the results were not very sensitive to these rate constants.

Nevertheless, given the uncertainty in some of the rate constants in the model, especially those for relaxation at low temperatures, and the simplistic assumption of how the release of heat affects the gas density, we assume an error of ±50% in the correction factors (expressed as a percentage) and we combine these errors with those estimated previously in the usual way to yield an estimate of 30% in the final values, k_1(corr.), of the rate constants. These are listed in the final column of Table 2.

Our values of k_1(corr.) are plotted against temperature in Figure 3, where they can be compared with previous experimental data at different, but higher, temperatures and with the theoretical estimates of Davidsson and Stenholm[38] and of Harding et al.[10c] The rate constants determined in the present work are lower, but not greatly lower, than those of Smith and Stewart[6] in the range of temperature where they overlap. This suggests an unidentified, but fairly small, source of systematic error in one or other set of experiments. The restrictions imposed by the CRESU method would appear to make these measurements more likely to suffer from such an error, but we have allowed, as best as is currently possible, for three such effects. At present, it seems safest to conclude that the rate constant for reaction R1 shows no appreciable variation with temperature in the range 142 to 39 K and we recommend a value for k_1 of

$(3.5 \pm 1.0) \times 10^{-11}$ cm^3 molecule^{-1} s^{-1} throughout this range of temperature.

Although the cold cores of dark ISCs reach lower temperatures than 39 K, usually having temperatures in the range 10−20 K, it seems inherently unlikely that k_1 will fall dramatically between 39 and 10 K. Certainly, the value of k_1 at 39 K precludes an activation energy as high as E_{act}/R of 80 K, which Viti et al.[23] suggested was needed if k_1 was to become sufficiently small to explain the low abundance of O_2 on the grounds of a low rate of reaction between OH and O(^{3}P) atoms. Nevertheless, our experiments do suggest that the value of k_1 used in chemical models of ISCs should be lowered by a factor of about four from that used most recently.

In Figure 3 we compare our experimental results, and those of some others, with the results of two of the many theoretical calculations on this reaction. Davidsson and Stenholm,[38] building on earlier work by Davidsson and Nyman,[39] used what they termed an "extended Langevin model", as well as classical trajectories to calculate values of $k_1(T)$. The calculations used the DMBE III potential energy surface of Varandas et al.[40] which includes chemical binding effects and for which the potential energy depends on both the separation of the collision partners OH and O and the angle (θ) between the OH internuclear axis and the line joining the centers of OH and O. A simple capture calculation then yields cross sections for combinations of collision energy and θ, and the rate constants are found by appropriate integrations over these two variables. Allowance is made for reaction occurring on only the $^2A''$ ground-state surface of HO_2, and this rather simple treatment gives moderate agreement with the experimental results. The curve shown in Figure 3 corresponds to the expression that they recommended for $k_1(T)$ having considered all their results.

Troe and co-workers have published several theoretical papers[10] on reactions R1 and R-1 over a number of years. In Figure 3, we display the results of the paper by Harding et al.[10c] In this work, the potential energy surface is characterized by high-level ab initio calculations. Then the rate constant for reaction is calculated using a combination of statistical adiabatic channel model (SACM) and classical trajectory methods. Once again, the calculated results are in rather good agreement with experiment, although the present results rather reduce the quality of that agreement, relative to the comparison of theory with the data of Smith and Stewart.[6]

Summary and Conclusions

In this paper, we have reported the first study in a CRESU apparatus of a reaction between two neutral, and unstable, free radicals: OH($X^2\Pi_\Omega$) and O(^3P_J). In the experiments, both of these species were formed photochemically by processes initiated by radiation at 157.6 nm from a F_2 excimer laser. Kinetic decays for the OH($X^2\Pi_\Omega$) radical were recorded using time-delayed laser-induced fluorescence: OH being excited in the (1, 0) band of the $A^2\Sigma^+ - X^2\Pi$ system at ca. 282 nm, fluorescence being observed in the (1, 1) and (0, 0) bands at ca. 310 nm. Analysis of the data allowed for the significant optical absorption of the photolysis laser beam by O_2 along the axis of the gas jet formed in the CRESU chamber. Further corrections to the derived rate constants, k_1(uncorr.), were then made to allow for both the significant increase in temperature and decrease in density as a result of heat released during the photochemical formation of O(^{3}P) atoms and for the formation and relaxation of OH radicals initially formed in vibrationally excited levels.

Once these corrections were applied, the rate constant, k_1(corr.), for the reaction between OH($X^2\Pi_\Omega$) and O(^3P_J) shows no significant variation in the temperature range between ca. 142 and 39 K and we derive a value of $(3.5 \pm 1.0) \times 10^{-11}$ cm^3 molecule^{-1} s^{-1} through this range of temperature. This result is lower, by a factor of less than two, than both the most complete theoretical calculations of the rate constant for this reaction, those of Troe and co-workers,[10] and the previous measurements of Smith and Stewart[6] at temperatures down to 158 K. Given the difficulty of both the experiments and the theoretical calculations, this moderate level of agreement seems fairly satisfactory.

The extension of kinetic measurements on this reaction to temperatures as low as 39 K has important astrochemical implications. We find no evidence that the rate constant starts to fall as the temperature is lowered to 39 K. Although this temperature remains higher than those found in the coldest cores in ISCs, it appears unlikely that the rate constant, k_1, will fall dramatically between 39 K and those temperatures of 10−20 K. Certainly, any activation energy must be appreciably less than the value ($E_{act}/R = 80$ K) that Viti et al.[23] suggested would be necessary to explain the low abundance of O_2 in ISCs. It seems as if the explanation for the low interstellar abundance of O_2 must be sought elsewhere than in the slow rate of the reaction between OH radicals and O(^3P_J) atoms at very low temperatures.

Acknowledgment. We are grateful to EPSRC for a research grant in support of this work. The work was also supported by a TMR Research network grant of the European Union, "Astrophysical chemistry: Experiments, calculations and astrophysical consequences of reactions at low temperatures" under Contract FMRX-CT97-0132 (DG12-MIHT). We thank Dr. Valery LePage for experimental help during the early stages of this work, and I.W.M.S. thanks Dr. David McCabe for useful correspondence regarding the relaxation of vibrationally excited OH and for permission to use his results on the relaxation of vibrationally excited OH by O_2. I.R.S. also thanks the European Union for a Marie Curie Chair under Contract MEXC-CT-2004-006734.

References and Notes

(1) Wayne, R. P. *Chemistry of Atmospheres: An Introduction to the Chemistry of the Atmospheres of Earth, the Planets, and their Satellites*, 3rd ed; Oxford University Press: Oxford, U.K., 2000.

(2) (a) Miller, J. A.; Kee, R. J.; Westbrook, C. K. *Annu. Rev. Phys. Chem.* **1990**, *41*, 345. (b) Miller, J. A. *Int. Symp. Combust.*, 26th; The Combustion Institute, Pittsburgh, PA, 1996; p 461.

(3) Smith, I. W. M.; Herbst E.; Chang, Q. *Mon. Not. R. Astronom. Soc.* **2004**, *350*, 323.

(4) Howard, M. J.; Smith, I. W. M. *Prog. Reac. Kinet.* **1983**, *12*, 55.

(5) (a) Howard, M. J.; Smith, I. W. M. *Chem. Phys. Lett.* **1980**, *69*, 40. (b) Howard, M. J.; Smith, I. W. M. *J. Chem. Soc., Faraday Trans. 2* **1981**, *77*, 997.

(6) Smith, I. W. M.; Stewart, D. W. A. *J. Chem. Soc., Faraday Trans.* **1994**, *90*, 3221.

(7) Lewis, R. S.; Watson, R. T. *J. Phys. Chem.* **1980**, *84*, 3495.

(8) Brune, W. H.; Schwab, J. J.; Anderson, J. G. *J. Phys. Chem.* **1983**, *87*, 4503.

(9) Robertson, R.; Smith, G. P. *Chem. Phys. Lett.* **2002**, *358*, 157.

(10) (a) Troe, J. *J. Phys. Chem.* **1986**, *90*, 3485. (b) Harding, L. B.; Maergoiz, A. I.; Troe, J.; Ushakov, V. G. *J. Chem. Phys.* **2000**, *113*, 11019. (c) Troe, J.; Ushakov, V. G. *J. Chem. Phys.* **2001**, *115*, 3621.

(11) (a) See page 166 in ref 1. (b) See page 547 in ref 1.

(12) (b) Herbst, E.; Klemperer, W. *Astrophys. J.* **1973**, 185, 505. (b) Viala, Y. P.; Walmsmey, C. M. *Astron. Astrophys.* **1976**, *50*, 1.

(13) The $N_J = 3_3 \rightarrow 1_2$ transition is estimated (see ref 14) to have a spontaneous decay rate of 8.5×10^{-9} s^{-1}

(14) (a) Goldsmith, P. F.; Snell, R. L.; Erickson, N. R.; Dickman, R. L.; Schloerb, F. P.; Irvine, W. M. *Astrophys. J.* **1985**, *289*, 613. (b) Liszt, H. S.; Bout, P. A. V. *Astrophys. J.* **1985**, *291*, 178. (c) Fuente, A.; Cernicharo, J.; Garciaburillo, S.; Tejero, J. *Astron. Astrophys.* **1993**, *275*, 558. (d) Green, S. *Nuovo Cimento Soc. Ital. Fis., C: Geophys. Space Phys.*

1985, *8*, 435. (d) Maréchal, P.; Pagani, L.; Langer, W. D.; Castets, A. *Astron. Astrophys.* **1997**, *318*, 252. (e) Pagani, L.; Langer, W. D.; Castets, A. *Astron. Astrophys.* **1993**, *274*, L13.

(15) (a) Combes, F.; Casoli, F.; Encrenaz, P.; Gerin, M.; Laurent, C. *Astron. Astrophys.* **1991**, *248*, 607. (b) Combes, F.; Wiklind, T. *Astron. Astrophys.* **1995**, *303*, L61. (c) Combes, F.; Wiklind, T.; Nakai, N. *Astron. Astrophys.* **1997**, *327*, L17.

(16) Olofsson, G.; Pagani, L.; Tauber, J.; Febvre, P.; Deschamps, A.; Encrenaz, P.; Floren, H. G.; George, S.; Lecomte, B.; Ljung, B.; Nordh, L.; Pardo, J. R.; Peron, I.; Sjoekvist, M.; Stegner, K.; Stenmark, L.; Ullberg, C. *Astron. Astrophys.* **1998**, *339*, L81.

(17) Goldsmith, P. F.; Melnick, G. J.; Bergin, E. A.; Howe, J. E.; Snell, R. L.; Neufeld, D. A.; Harwit, M.; Ashby, M. L. N.; Patten, B. M.; Kleiner, S. C.; Plume, R.; Stauffer, J. R.; Tolls, V.; Wang, Z.; Zhang, Y. F.; Erickson, N. R.; Koch, D. G.; Schieder, R.; Winnewisser, G.; Chin, G. *Astrophys. J.* **2000**, *539*, L123.

(18) Pagani, L.; Olofsson, A. O. H.; Bergman, P.; Bernath, P.; Black, J. H.; Booth, R. S.; Buat, V.; Crovisier, J.; Curry, C. L.; Encrenaz, P. J.; Falgarone, E.; Feldman, P. A.; Fich, M.; Floren, H. G.; Frisk, U.; Gerin, M.; Gregersen, E. M.; Harju, J.; Hasegawa, T.; Hjalmarson, A.; Johansson, L. E. B.; Kwok, S.; Larsson, B.; Lecacheux, A.; Liljestrom, T.; Lindqvist, M.; Liseau, R.; Mattila, K.; Mitchell, G. F.; Nordh, L. H.; Olberg, M.; Olofsson, G.; Ristorcelli, I.; Sandqvist, A.; von Scheele, F.; Serra, G.; Tothill, N. F.; Volk, K.; Wiklind, T.; Wilson, C. D. *Astron. Astrophys.* **2003**, *402*, L77.

(19) Liseau, R. and the Odin team *Proc. IAU Symp.* 2005, *231*, in press.

(20) Casu, S.; Cecchi-Pestellini, C.; Aiello, S. *Mon. Not. R. Astron. Soc.* **2001**, *325*, 826.

(21) Spaans, M.; Van Dishoeck, E. F. *Astrophys. J.* **2001**, *548*, L217.

(22) Roberts, H.; Herbst, E. *Astron. Astrophys.* **2002**, *395*, 233.

(23) Viti, S.; Roueff, E.; Hartquist, T. W.; des Forets, G. P.; Williams, D. A. *Astron. Astrophys.* **2001**, *370*, 557.

(24) Bergin, E. A.; Melnick, G. J.; Stauffer, J. R.; Ashby, M. L. N.; Chin, G.; Erickson, N. R.; Goldsmith, P. F.; Harwit, M.; Howe, J. E.; Kleiner, S. C.; Koch, D. G.; Neufeld, D. A.; Patten, B. M.; Plume, R.; Schieder, R.; Snell, R. L.; Tolls, V.; Wang, Z.; Winnewisser, G.; Zhang, Y. F. *Astrophys. J.* **2000**, *539*, L129.

(25) Wilson, C. D.; Olofsson, A. O. H.; Pagani, L.; Booth, R. S.; Frisk, U.; Hjalmarson, A.; Olberg, M.; Sandqvist, A. *Astron. Astrophys.* **2005**, *433*, L5.

(26) Millar, T. J.; Farquhar, P. R. A.; Willacy, K. *Astron. Astrophys. Suppl.* **1997**, *121*, 139.

(27) James, P. L.; Sims, I. R.; Smith, I. W. M.; Alexander, M. H.; Yang, M. *J. Chem. Phys.* **1998**, *109*, 3882.

(28) (a) Gibson, S. T.; Gies, H. P. F.; Blake, A. J.; McCoy, D. G.; Rogers, P. J. *J. Quant. Spectrosc. Radiat. Trans*fer **1983**, *30*, 385. They have measured absorption cross-sections for O_2 over the range 140 nm to 174 nm and at 295 and 575 K. At 157.6 nm and at 295 K, they found $\sigma_{O_2} = 6.47 \times 10^{-18}$ cm^2. They computed virtually no dependence on temperature down to 40 K, consistent with the very minor change in vibrational populations over this temperature range. (b) More recently, Yoshino and co-workers (personal communication) have measured absorption cross-sections for O_2 over a range of wavelengths in the VUV. Their measurements yield a value of σ_{O_2} at $\lambda = 157.6$ nm of 5.94×10^{-18} cm^2. This is the value that we have employed in calculating the concentrations of O(^{3}P) atoms.

(29) This correction was originally introduced into the analysis in preliminary experiments that were conducted before the introduction of unstable optics in the photolysis laser. These optics greatly reduced the need for this correction. After the introduction of the unstable resonator optics, the experiments measuring changes in the LIF signal in mixtures containing H_2O, but no O_2, gave values of $|\alpha|$ that were, in only one case, >1 m^{-1}.

(30) Atkinson, R.; Baulch, D. L.; Cox, R. A.; Crowley, J. N.; Hampson, R. F.; Hynes, R. G.; Jenkin, M. E.; Rossi, M. J.; Troe, J. *Atmos. Chem. Phys.* **2004**, *4*, 1461.

(31) Hwang, D. W.; Yang, Xuefeng; Yang, Xueming. *J. Chem. Phys.* **1999**, *110*, 4119.

(32) (a) Gericke, K.-H.; Comes, F. J.; Levine, R. D. *J. Chem. Phys.* **1981**, *74*, 6106. (b) Cleveland, C. B.; Wiesenfeld, J. R. *J. Chem. Phys.* **1992**, *96*, 248.

(33) FACSIMILE for Windows, AEA Technology plc, U.K.

(34) (a) Carace, F.; de Petris, G.; Pepi, F.; Troiani, A. *Science* **1999**, *285*, 81. (b) Denis, P. A.; Kieninger, M.; Ventura, O. N.; Cachau, R. E.; Dierckson, G. H. F. *Chem. Phys. Lett.* **2002**, *365*, 440. (c) Suma, K.; Sumiyoshi, Y.; Endo, Y. *Science* **2005**, *308*, 1885.

(35) D'Ottone, L.; Bauer, D.; Campuzano-Jost, P.; Fardy, M.; Hynes, A. J. *Phys. Chem. Chem. Phys.* **2004**, *6*, 4276.

(36) (a) Rensberger, K. J.; Jeffries, J. B.; Crosley, D. R. *J. Chem. Phys.* **1989**, *90*, 2174. (b) Dodd, J. A.; Lipson, S. J.; Blumberg, W. A. M. *J. Chem. Phys.* **1990**, *92*, 3387. (c) Dodd, J. A.; Lipson, S. J.; Blumberg, W. A. M. *J. Chem. Phys.* **1991**, *95*, 5752.

(37) McCabe, D. Ph.D. Thesis, University of Colorado, Boulder, 2004.

(38) Davidsson, J.; Stenholm, L. G. *Astron. Astrophys.* **1990**, *230*, 504.

(39) (a) Davidsson, J.; Nyman, G. *Chem. Phys.* **1988**, *125*, 171. (b) Davidsson, J.; Nyman, G. *J. Chem. Phys.* **1990**, *92*, 2407. (c) Nyman, G.; Davidsson, J. *J. Chem. Phys.* **1990**, *92*, 2415.

(40) Varandas, A. J. C.; Brandão, J.; Quintales, L. A. M.; *J. Phys. Chem.* **1988**, *92*, 3732.